Identification of tyrosylprotein sulfotransferase in *Arabidopsis*

Ryota Komori, Yukari Amano, Mari Ogawa-Ohnishi, and Yoshikatsu Matsubayashi[1]

Graduate School of Bio-Agricultural Sciences, Nagoya University, Chikusa, Nagoya 464-8601, Japan

Edited by Alessandro Vitale, Consiglio Nazionale delle Ricerche, Milan, Italy, and accepted by the Editorial Board June 25, 2009 (received for review March 13, 2009)

Tyrosine sulfation is a posttranslational modification common in peptides and proteins synthesized by the secretory pathway in most eukaryotes. In plants, this modification is critical for the biological activities of a subset of peptide hormones such as PSK and PSY1. In animals, tyrosine sulfation is catalyzed by Golgi-localized type II transmembrane proteins called tyrosylprotein sulfotransferases (TPSTs). However, no orthologs of animal TPST genes have been found in plants, suggesting that plants have evolved plant-specific TPSTs structurally distinct from their animal counterparts. To investigate the mechanisms of tyrosine sulfation in plants, we purified TPST activity from microsomal fractions of *Arabidopsis* MM2d cells, and identified a 62-kDa protein that specifically interacts with the sulfation motif of PSY1 precursor peptide. This protein is a 500-aa type I transmembrane protein that shows no sequence similarity to animal TPSTs. A recombinant version of this protein expressed in yeast catalyzed tyrosine sulfation of both PSY1 and PSK precursor polypeptide in vitro, indicating that the newly identified protein is indeed an *Arabidopsis* (At)TPST. AtTPST is expressed throughout the plant body, and the highest levels of expression are in the root apical meristem. A loss-of-function mutant of *AtTPST* displayed a marked dwarf phenotype accompanied by stunted roots, pale green leaves, reduction in higher order veins, early senescence, and a reduced number of flowers and siliques. Our results indicate that plants and animals independently acquired tyrosine sulfation enzymes through convergent evolution.

Golgi | peptide hormone | posttranslational modification | tyrosine sulfation | sulfated tyrosine

Tyrosine sulfation is a common posttranslational modification found in peptides and proteins synthesized through the secretory pathway of most eukaryotes, including higher plants. This modification is thought to be mediated by an enzyme, tyrosylprotein sulfotransferase (TPST), which catalyzes the transfer of sulfate from 3′-phosphoadenosine 5′-phosphosulfate (PAPS) to the phenolic group of tyrosine (1). To date, 2 tyrosine sulfated peptide hormones, PSK and PSY1, have been found in plants. PSK is a 5-aa secreted peptide containing 2 sulfated tyrosines, and was initially identified as a growth-promoting factor involved in the "density effect" in plant cell cultures (2). PSK is recognized by a membrane-localized leucine-rich repeat (LRR) receptor kinase, PSKR1, and promotes cellular proliferation at nanomolar concentrations (3). Disruption of PSKR1 and its 2 homologs in *Arabidopsis* causes pleiotropic growth defects such as short roots, smaller leaves, and early senescence (4). PSY1 is an 18-aa secreted glycopeptide containing 1 sulfated tyrosine, and was identified by exhaustive analysis of tyrosine sulfated peptides in plant cell culture media (4). PSY1 also promotes cellular proliferation at nanomolar concentrations. There is evidence that one PSKR1 homolog is involved in the recognition of PSY1 (4). Both PSK and PSY1 are generated from longer precursor polypeptides through proteolytic processing. As with tyrosine-sulfated peptide hormones in animals, tyrosine-sulfation of PSK and PSY1 is critical for their function.

In mice and humans, tyrosine sulfation is mediated by 2 structurally related proteins, TPST-1 and TPST-2 (5, 6). TPSTs are ≈50-kDa type II transmembrane proteins that reside in the *trans*-Golgi network and have luminally oriented catalytic domains. Their orthologs have been found in invertebrates such as *Caenorhabditis elegans* and *Drosophila melanogaster* (1). However, sequence similarity searches have not identified any orthologs of TPST-1 and TPST-2 in *Arabidopsis* or other plant species. Nevertheless, significant TPST activity has been detected in microsomal fractions of various plant species (7), suggesting that plant TPST has evolved in a manner distinct from its animal counterpart.

Detailed analysis of the substrate specificity of plant TPST suggests that this enzyme recognizes tyrosine residues located near multiple acidic amino acids (7). Indeed, precursor polypeptides of PSK contain multiple acidic amino acids upstream from the tyrosine (8). Similarly, there are 3 acidic amino acids within 5 residues of the sulfated tyrosine of *Arabidopsis* PSY1 precursor polypeptide (4). Based on the known substrate specificity of TPST and sequence motifs for tyrosine sulfation in plants, we expected that synthetic oligopeptides containing a tyrosine residue and an acidic amino acid motif would specifically interact with the plant TPST with sufficient affinity to allow purification of the enzyme. Affinity purification is a powerful method where usually only 1 purification step is required to obtain the target protein with high homogeneity. Here, we show affinity purification and molecular cloning of *Arabidopsis* (At)TPST by using a PSY1 acidic motif oligopeptide as an affinity probe. We also provide evidence that tyrosine sulfation is important for plant development, based on a phenotypical analysis of a loss-of-function mutant of AtTPST.

Results

PSY1 Precursor Polypeptide Is an Efficient Substrate for AtTPST. To establish an efficient assay for TPST activity in plants, we used the *Arabidopsis* PSY1 precursor polypeptide (pPSY1) as a substrate because of the presence of a clear-cut acidic motif adjacent to the tyrosine residue (Fig. S1*A*). The pPSY1 (excluding the signal peptide) was expressed as a GST fusion protein in *Escherichia coli* and used to test whether TPST activity in *Arabidopsis* microsomal fractions can be detected with GST-pPSY1. Incubation of GST-pPSY1 with [^{35}S]PAPS in the presence of solubilized microsomal fractions prepared from *Arabidopsis* MM2d cells (L*er* ecotype) resulted in the incorporation of considerable radioactivity into a 32-kDa band corresponding to GST-pPSY1 (Fig. S1*B*). A mutated substrate, in which Tyr^{49} of

Author contributions: Y.M. designed research; R.K., Y.A., M.O.-O., and Y.M. performed research; R.K., Y.A., M.O.-O., and Y.M. analyzed data; and Y.M. wrote the paper.

The authors declare no conflict of interest.

This article is a PNAS Direct Submission. A.V. is a guest editor invited by the Editorial Board.

See Commentary on page 14741.

[1]To whom correspondence should be addressed. E-mail: matsu@agr.nagoya-u.ac.jp.

This article contains supporting information online at www.pnas.org/cgi/content/full/0902801106/DCSupplemental.

Table 1. Purification of *Arabidopsis* TPST

Purification step	Total protein, mg	Total activity, units	Specific activity, units/mg	Yield, %	Purification, fold
MM2d microsomal membranes	1,500	25,000	16.7	100	1.0
TX-100 solubilization	1,200	22,500	18.8	90	1.1
pPSY1[43–57]-Sepharose column	<0.1	3,750	>37,500	15	>2,250
Hydroxyapatite column	0.018	2,750	153,000	11	9,170

PSY1 was substituted by Ala (GST-[Y49A]pPSY1), was not sulfated under the same conditions, indicating that the observed reaction is indeed tyrosine sulfation (Fig. S1*B*).

To further test whether shorter peptide fragments corresponding to the acidic motif region of pPSY1 also act as an efficient substrate for TPST, we chemically synthesized a 15-aa acidic motif peptide in which K^{57} is replaced by Cys, and cross-linked the peptide to BSA via the C-terminal Cys residue in the peptide. This synthetic substrate, BSA-pPSY1[43-57], was also efficiently sulfated by the TPST activity in solubilized *Arabidopsis* microsomal fractions (Fig. S1*B*). These results indicate that this acidic motif peptide is sufficient to interact with TPST in the presence of PAPS, even when the C-terminal residue of the substrate peptide is cross-linked to a larger molecule.

Affinity Purification of AtTPST Using a PSY1 Precursor Peptide Column. To purify AtTPST, we first synthesized a 15-aa acidic motif peptide and immobilized it onto Sepharose via a C-terminal Lys residue. This pPSY1[43-57]-Sepharose was used as an affinity matrix for TPST purification. Solubilized microsomal fractions (1,200 mg protein equivalent) prepared from *Arabidopsis* MM2d cells were applied to the pPSY1[43-57]-Sepharose column in the presence of 3′-phosphoadenosine 5′-phosphate (PAP). PAP is known to bind sulfotransferases competitively with PAPS, and promotes the formation of a stable enzyme-substrate ternary complex (9). The column was washed with buffer containing PAP and eluted with the same buffer devoid of PAP. Enzyme activity eluted from the pPSY1[43-57]-Sepharose column was further purified by using a hydroxyapatite column, and TPST active fractions were pooled. After 2 steps of purification, enzyme activity was enriched 9,170-fold, with a yield of 11% (Table 1). Purified proteins were further concentrated by ultrafiltration followed by acetone precipitation, and analyzed by SDS/PAGE. After fluorescent staining of the gel, several ≈60-kDa protein bands were detected (Fig. 1*A*).

To determine which protein band corresponded to TPST, we performed photoaffinity labeling by using a photoactivatable 4-azidosalicylic acid (ASA) derivative of the pPSY1[43-57] peptide, (ASA-pPSY1[43-57]). Because sulfur-containing amino acids decrease chloramine-T-mediated radioiodination, Met^{43} was replaced by Ala in the photoaffinity probe. Incubation of the purified TPST fractions with [^{125}I]ASA-pPSY1[43-57] followed by UV irradiation resulted in the labeling of a 62-kDa band (Fig. 1*B*). This cross-linking reaction was inhibited by the addition of excess unlabeled pPSY1[43-57], indicating that the labeling is specific. These results show that this 62-kDa protein is a possible candidate for an AtTPST.

Molecular Cloning of AtTPST. The 62-kDa band was excised and subjected to in-gel tryptic digestion. Subsequent peptide mass fingerprinting (PMF) analysis revealed that the MS signals matched 7 internal tryptic fragments of At1g08030 protein (Fig. 1 *C* and *D*). Full-length At1g08030 cDNA was isolated by RT-PCR and 3′-RACE by using total RNA from *Arabidopsis* MM2d cells. The current annotation of the C-terminal region of At1g08030 in The *Arabidopsis* Information Resource (TAIR)

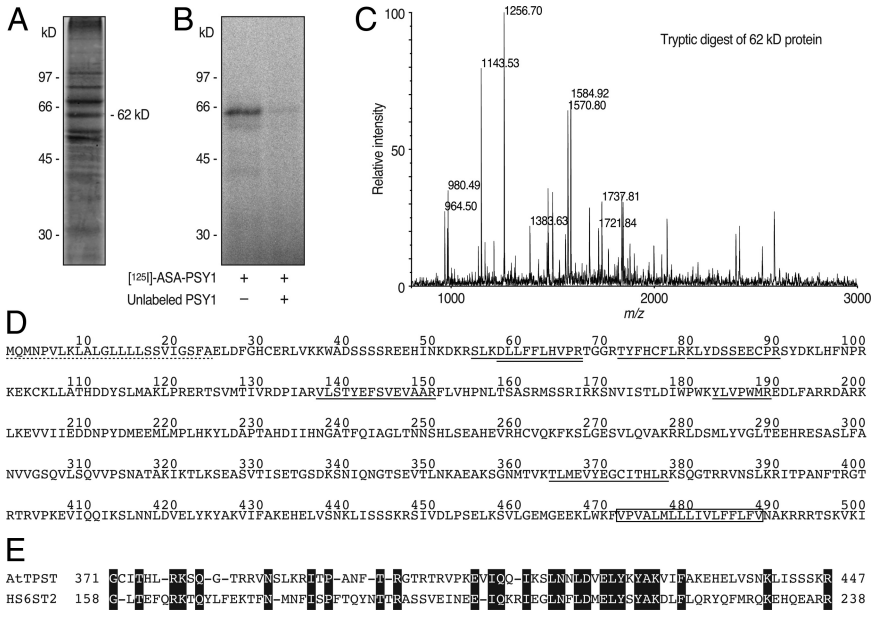

Fig. 1. Identification of AtTPST. (*A*) SDS/PAGE profile of partially purified AtTPST. (*B*) Photoaffinity labeling of AtTPST by [^{125}I]ASA-pPSY1[43-57]. A 62-kDa protein was specifically labeled by the photoaffinity ligand. (*C*) MALDI TOF-MS spectrum of the tryptic digest of the 62-kDa protein. (*D*) PMF analysis revealed that 9 MS signals matched 7 internal tryptic fragments of the At1g08030 protein. Matched fragments are underlined. Two fragments show double MS signals due to the partial oxidation of a Met residue. The putative signal peptide is underlined with a dashed line, and the transmembrane domain is boxed. (*E*) Schematic representation of the alignment between AtTPST and human heparan sulfate 6-*O*-sulfotransferase 2 (HS6ST2).

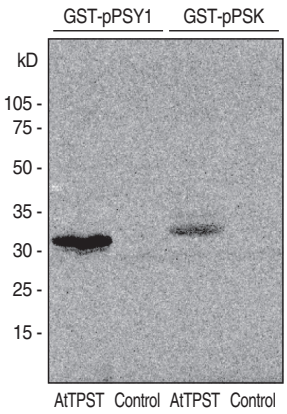

Fig. 2. Tyrosine sulfation activities of recombinant AtTPST expressed in yeast. GST-pPSY1 or GST-pPSK was incubated with [^{35}S]PAPS in the presence of solubilized yeast microsomal fractions expressing AtTPST, or empty vector (control), and analyzed by SDS/PAGE followed by autoradiography.

was found to be incorrect. The correct ORF encodes a 500-aa protein containing a signal peptide at the N-terminal and a single transmembrane region near the C terminus (Fig. 1*D*). This deduced protein has 6 potential *N*-glycosylation sites (Asn-X-Ser/Thr), which account for the discrepancy between the molecular size of the predicted protein (57 kDa) and the purified protein (62 kDa). This protein has no sequence similarity to human TPSTs, but contains a region near the C terminus that has similarity to the human heparan sulfate, 6-*O*-sulfotransferase 2 (Fig. 1*E*). No other specific protein domains or features could be identified. At1g08030 appears to be present as a single gene in *Arabidopsis*.

Functional Expression of AtTPST in Yeast. To verify that the isolated cDNA indeed encodes a functional TPST, the full-length cDNA was expressed in yeast under the control of the *GAL1* promoter. After induction by galactose, microsomal fractions of the recombinant yeast were collected and tested for TPST activity. After incubation of GST-pPSY1 with [^{35}S]PAPS in the presence of solubilized microsomal fractions prepared from the recombinant yeast, significant incorporation of radioactivity into the 32-kDa band corresponding to GST-pPSY1 was detected (Fig. 2). In contrast, no TPST activity was detected in the microsomal fractions derived from yeast transformed with empty vector. Recombinant protein also catalyzed the tyrosine sulfation of *Arabidopsis* PSK precursor polypeptide expressed as a GST fusion protein (GST-pPSK) (Fig. 2). These results indicate that the cDNA (At1g08030) encodes a functional TPST in *Arabidopsis*.

Tissue Expression Pattern and Subcellular Localization of AtTPST. To investigate the expression pattern of *AtTPST* at the tissue level, we transformed *Arabidopsis* with an *AtTPST* promoter *GUS* fusion construct (*AtTPSTpro*:*GUS*). Histochemical staining for GUS in whole plants detected GUS activity in all plant tissues, with the highest levels of expression in root apical meristem (RAM) (Fig. 3 *A* and *B*). High levels of expression of *GUS* were also observed in the lateral root primordia and vascular tissues.

To analyze the subcellular localization of AtTPST, a chimeric protein, GFP-AtTPST, was transiently expressed under the 35S promoter in *Arabidopsis* protoplasts. Because AtTPST has consecutive basic amino acids at the C-terminal that may function as a subcellular targeting signal, we inserted GFP between the N-terminal signal peptide and the core region of AtTPST. Laser confocal microscopic analysis revealed that transformed cells displayed a punctate pattern of GFP fluorescence, suggesting a Golgi-localization (Fig. 3*C*). To confirm that these fluorescent structures are Golgi stacks, we tested their sensitivity to brefeldin A (BFA). BFA induces fusion of Golgi with ER membranes and collapses the Golgi into the ER. When transformed protoplasts were incubated with BFA for 2 h, GFP fluorescence was distributed in ER network-like structures (Fig. 3*D*). These results indicate that AtTPST is localized in the Golgi apparatus, most likely in *cis*-Golgi. This subcellular localization was further confirmed by colocalization of GFP-AtTPST with a known *cis*-Golgi marker, mRFP-SYP31 (Fig. 3 *E* and *F*) (10).

Characterization of *AtTPST* Loss-of-Function Mutant. To determine the *in planta* function of *AtTPST*, a mutant line (*tpst-1*) homozygous for a T-DNA insertion in the *AtTPST* gene (SALK_009847) was isolated. Sequencing of the T-DNA/genomic DNA boundaries revealed a single insertion in exon 5 with a 22-bp deletion in the insertion border region (Fig. 4*A*). This T-DNA insertion, which leads to the absence of full-length *AtTPST* transcripts, was confirmed by RT-PCR (Fig. 4*B*). We also confirmed the absence of TPST activity in the microsomal fractions of *tpst-1* (Fig. 4*C*).

Homozygous *tpst-1* displayed pleiotropic growth defects. Seedlings of *tpst-1* had stunted roots and smaller cotyledons compared with the WT (Fig. 4 *D* and *E*). Confocal microscopy

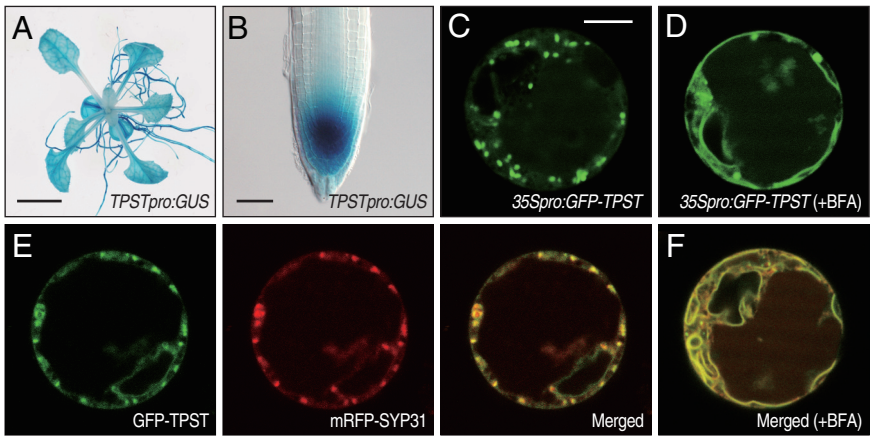

Fig. 3. Tissue expression pattern and subcellular localization of AtTPST. (*A*) Histochemical staining of a 14-day-old *Arabidopsis* plant transformed with the *AtTPSTpro*:*GUS* gene. (Scale bar, 5 mm.) (*B*) Close-up of RAM in *A*. (Scale bar, 50 μm.) (*C*) Subcellular localization of the GFP-AtTPST fusion protein transiently expressed in *Arabidopsis* protoplasts. (Scale bar, 10 μm.) (*D*) Effect of BFA treatment (50 μg/mL) on GFP-AtTPST localization. (*E*) Colocalization of GFP-AtTPST with *cis*-Golgi marker, mRFP-SYP31. (*F*) Colocalization of GFP-AtTPST with mRFP-SYP31 after BFA treatment.

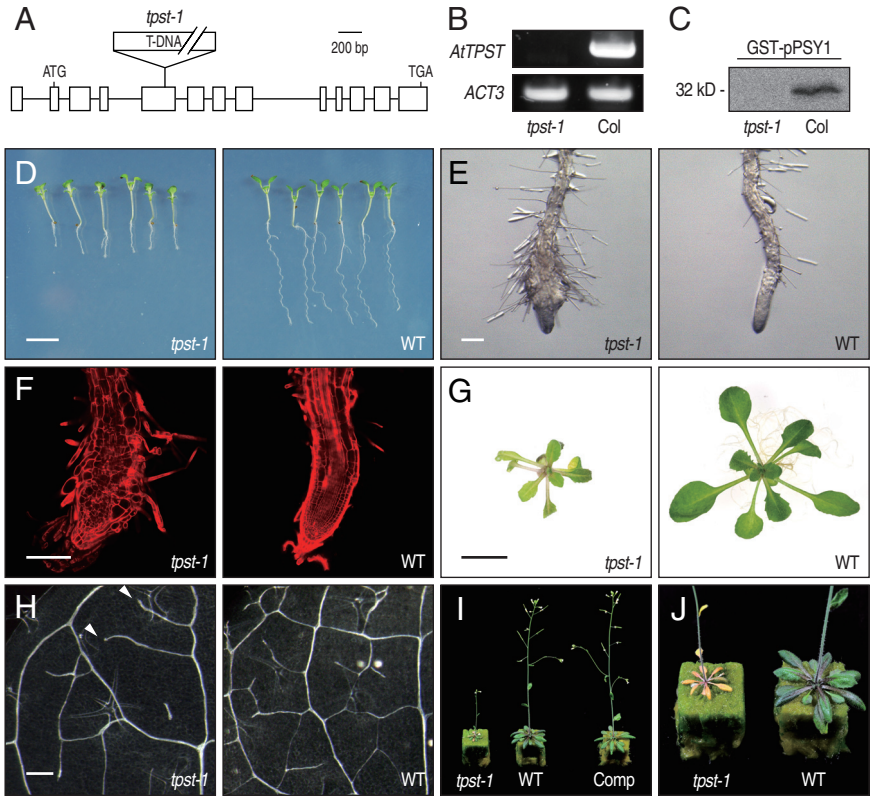

Fig. 4. Phenotypes of a loss-of-function mutant of *AtTPST*. (*A*) Schematic map of the T-DNA insertion site of *tpst-1* (SALK_009847). (*B*) Absence of *AtTPST* transcripts in homozygous *tpst-1* plants. RT-PCR analyses were performed on total RNA extracted from *tpst-1* or WT plants by using primers specific for *AtTPST* or for the *Arabidopsis ACT3* gene (used as a control). (*C*) Absence of TPST activities in homozygous *tpst-1* plants. GST-pPSY1 was incubated with [^{35}S]PAPS in the presence of solubilized *Arabidopsis* microsomal fractions derived from *tpst-1* or WT plants and analyzed by SDS/PAGE followed by autoradiography. (*D*) Vertically grown 7-day-old seedlings of *tpst-1* and WT. (Scale bar, 5 mm.) (*E*) Close-up of RAM in *D*. (Scale bar, 200 μm.) (*F*) Confocal images of RAM in *D* stained with propidium iodide. (Scale bar, 200 μm.) (*G*) Three-week-old plants of *tpst-1* and WT grown on B5 agar plates. (Scale bar, 1 cm.) (*H*) First leaf of *tpst-1* and WT cleared by chloral hydrate. In *tpst-1* leaves, secondary veins often do not close (indicated by arrows). (Scale bar, 200 μm.) (*I*) Four-week-old plants of *tpst-1*, WT, and *tpst-1* complemented with *AtTPST*. (*J*) Five-week-old plants of *tpst-1* and WT.

of the roots revealed that *tpst-1* has an abnormally shaped RAM due to disorganized cell division and expansion (Fig. 4*F*). At 15 days after germination, the leaves of the *tpst-1* plants are small and pale green, the number of higher order veins is reduced, and the secondary veins often do not close (Fig. 4 *G* and *H*). At the flowering stage, *tpst-1* has smaller rosettes, tiny leaves showing early senescence, shorter inflorescence, and a reduced number of flowers and siliques (Fig. 4 *I* and *J*). The fertility and seed set of *tpst-1* are normal.

Transformation of *tpst-1* homozygous plants with the transgene containing *35S:AtTPST* fully complemented the mutant phenotypes, demonstrating that these phenotypes are caused by the disruption of *AtTPST* (Fig. 4*I*). These *tpst-1* phenotypes indicate important and pleiotropic roles of tyrosine sulfation in plant growth and development.

Discussion

We have affinity-purified AtTPST from microsomal fractions of *Arabidopsis* MM2d cells and shown it to be a previously undescribed 62-kDa Golgi-localized transmembrane protein. Possible AtTPST orthologs were found in other higher plants such as rice and maize, in the moss *Physcomitrella patens*, and in the green alga *Chlamydomonas reinhardtii*, but not in yeast or animals. Indeed, AtTPST shows no sequence similarity with animal TPSTs, even though both enzymes catalyze identical sulfate transfer reactions by using the same cosubstrate, PAPS. AtTPST is a 500-aa glycoprotein that migrates at 62 kDa on SDS/PAGE, whereas human TPST-1 is a 370-aa glycoprotein that migrates at 54 kDa (6). Also, AtTPST is a type I transmembrane protein in which the transmembrane domain is located close to the C terminus, whereas human TPST-1 is a type II transmembrane protein in which the transmembrane domain is located close to the N terminus. This structural diversity strongly suggests that the *AtTPST* gene has evolved from an ancestral gene distinct from that of animal TPSTs. Together, our results suggest that plants and animals independently acquired enzymes for tyrosine sulfation through convergent evolution.

Our sulfation assay confirmed that AtTPST catalyzes tyrosine sulfation of both PSY1 and PSK precursor polypeptides in vitro, indicating the broad substrate sequence specificity of this enzyme. It has been reported that the minimum requirement for tyrosine sulfation in plants is the presence of Asp immediately N-terminal to Tyr, and that multiple acidic amino acids near this Tyr significantly enhance sulfation (7). Structurally, the Tyr residue in PSY1 is surrounded by multiple acidic amino acids (-EDYGD-), whereas the acidic region in PSK precursor polypeptides is located >10 residues upstream from Tyr. Because recombinant AtTPST catalyzed tyrosine sulfation of the PSY1 precursor polypeptide more efficiently than it did the PSK precursor, we speculate that closer proximity of the acidic region to the Tyr residue markedly enhances association with AtTPST. In evolutionary terms, it is quite interesting that the substrate specificity of plant TPST is fairly similar to that of animal TPSTs, despite the total lack of sequence similarity between the 2 enzymes.

AtTPST is a single copy gene that is widely expressed in many tissues in *Arabidopsis*, including meristem regions. We confirmed the absence of endogenous TPST activity in the microsomal fractions of the *tpst-1* mutant, indicating that AtTPST is indeed a unique protein in *Arabidopsis*. A loss-of-function mutant of *AtTPST* displayed a marked dwarf phenotype accompanied by stunted roots, abnormally shaped RAM, pale green leaves, reduction in higher order veins, early senescence, and a reduced number of flowers and siliques. These phenotypes are evidently more severe than those of the *AtPSKR1 AtPSKR2* At1g72300 triple loss-of-function mutant, which lacks PSK receptors and a putative receptor for PSY1, each of which belong to the LRR receptor kinase subfamily X. In particular, the abnormally shaped RAM phenotype was specific for *tpst-1* and was not observed in the above triple mutant. Taking the broad substrate sequence specificity of AtTPST into consideration, we predict the presence in *Arabidopsis* of as yet uncharacterized tyrosine-sulfated peptides or proteins involved in plant growth and development, especially in root development. Further identification of tyrosine-sulfated peptides or proteins underlying *tpst-1* defects will uncover previously undescribed intercellular signals important for plant development, and will facilitate our understanding of the role of tyrosine sulfation in multicellular organisms, including plants.

Materials and Methods

Preparation of *Arabidopsis* Microsomal Membranes. MM2d *Arabidopsis* cell suspension culture was maintained as described (11). Seven-day-old MM2d cells (200-g fresh weight) were homogenized in a Waring blender (20,000 rpm for 5 min) at 4 °C in 200 mL of 25 mM Tris·HCl (pH 7.0) buffer containing 10 mM $MgCl_2$, 2 mM DTT, 2 μM leupeptin, 2 mM PMSF and 250 mM sucrose. The slurry was filtered through Miracloth and centrifuged at 10,000 $\times$ *g* for 15 min at 4 °C. The supernatant was further centrifuged at 100,000 $\times$ *g* for 30 min at 4 °C to give a pellet of microsomal membranes.

Preparation of GST-pPSY1, GST-[Y49A]pPSY1, and BSA-pPSY1[43-57]. A PSY1 precursor polypeptide (excluding the signal peptide) (4) was expressed as a GST fusion protein in *E. coli by using* pGEX-4T-3 expression vector (GE Healthcare). Expressed GST-pPSY1 was purified by using a glutathione-Sepharose column according to the manufacturer's protocol. By the same procedure, an AtPSK2 precursor polypeptide (excluding the signal peptide) (8) was expressed as a GST fusion protein in *E. coli by using* pGEX-4T-3 expression vector. For the expression of GST-[Y49A]pPSY1, the Y49A mutation was introduced into the PSY1 cDNA by PCR mutagenesis, and the resulting DNA fragment was introduced into the pGEX-4T-3 expression vector.

For the preparation of BSA-pPSY1[43-57], 5.0 mg of partially protected Fmoc-MVNVEDYGDPSANPC peptide prepared by solid-phase synthesis (ABI 433A) was conjugated to 10 mg of BSA by using the heterobifunctional cross-linker, *m*-maleimidobenzoyl-*N*-hydroxysuccinimidyl ester (MBS). The cross-linked material was treated with 50% piperidine for 30 min to remove the Fmoc groups, and then the conjugate was purified by gel-filtration.

Detection of TPST Activity. *Arabidopsis* microsomal membranes (30 μg) or purified samples were added in 25 μL of 50 mM Tris·HCl (pH 8.0) buffer containing 150 mM NaCl, 1.0% Triton X-100 and 5 μg of GST-pPSY1 (or GST-pPSK). After addition of 10 kBq of [^{35}S]PAPS (PerkinElmer), the reaction mixture was incubated at 30 °C for 2.5 h and separated by SDS/PAGE on a 12.5% acrylamide gel. The dried gels were exposed to a bio-imaging plate (MS 2025; Fujifilm) for 2 days, then the plates were analyzed by using an imaging plate reader and bio-imaging analyzer (BAS 5000; Fujifilm). For sulfation of BSA-pPSY1[43-57], *Arabidopsis* microsomal membranes (30 μg) were added in 25 μL of the reaction buffer containing 5 μg of BSA-pPSY1[43-57]. One unit of activity was defined as 1 fmol of product formed per minute.

Preparation of Affinity Column. For the preparation of the pPSY1[43-57]-Sepharose column, 35 mg (18.8 μmol) of Fmoc-MVNVEDYGDPSANPK prepared by solid-phase synthesis was dissolved in 5 mL of 50% acetonitrile containing 1% $NaHCO_3$ and coupled to 5 mL prepacked Hi-Trap NHS activated Sepharose (GE Healthcare) at 25 °C for 16 h. After blocking the unreacted NHS groups by using 5 mL of 0.2 M ethanolamine, the ligand-coupled Sepharose was treated with 5 mL of piperidine:acetonitrile:water (2:1:1) for 10 min to remove the Fmoc groups. Coupling efficiency was 5.5 μmol peptide per 5 mL Sepharose, as determined by measuring the absorbance of the released fluorene derivative at 301 nm. The column was thoroughly washed with 50% acetonitrile and water before use.

Affinity Purification of TPST. *Arabidopsis* microsomal membranes derived from MM2d cells (750 mg protein) were solubilized in 120 mL of 50 mM Tris·HCl (pH 8.0) buffer containing 150 mM NaCl, 200 μM PAP and 1.0% Triton X-100. Solubilized materials were centrifuged at 100,000 $\times$ *g* for 30 min at 4 °C, and the supernatants were applied to the pPSY1[43-57]-Sepharose column (5 mL) at a flow rate of 0.5 mL/min at 4 °C. After washing with 15 mL of 50 mM Tris·HCl (pH 8.0) buffer containing 150 mM NaCl, 200 μM PAP and 0.1% Triton X-100, the column was eluted with 400 mL of 50 mM Tris·HCl (pH 8.0) buffer containing 150 mM NaCl and 0.1% Triton X-100 (devoid of PAP). Two independent purification experiments recovered a total of 400 mL of TPST-active fractions from 1,500 mg of MM2d microsomal membranes. The active fractions were further applied to a 1-mL column of MacroPrep Ceramic Hydroxyapatite Type I (Bio-Rad laboratories) at a flow rate of 1.5 mL/min at 4 °C. The column was washed with 5 mL of 50 mM Tris·HCl (pH 8.0) buffer containing 150 mM NaCl and 0.1% Triton X-100, and eluted with 20 mL of 200 mM NaH_2PO_4-NaOH (pH 8.0) buffer containing 150 mM NaCl and 0.1% Triton X-100. Active fractions (1 mL), as determined by the TPST assay, were concentrated to $\approx$100 μL by ultrafiltration (Ultrafree-MC 5,000 NMWL filter unit; Millipore) and the proteins were precipitated by addition of 1 mL of acetone at $-$20 °C for 16 h. The precipitated proteins were reduced with DTT, alkylated with iodoacetoamide, and analyzed by SDS/PAGE using 10% gels.

Preparation of Photoactivatable [^{125}I]ASA-pPSY1[43-57]. The Fmoc-protected [M43A]pPSY1[43-57] peptide derivative Fmoc-AVNVEDYGDPSANPK was synthesized by Fmoc chemistry using a peptide synthesizer. ASA succinimidyl ester [1.7 mg (6 μmol); Pearce], Fmoc-AVNVEDYGDPSANPK [5.4 mg (3 μmol)], and $NaHCO_3$ (5.0 mg) were dissolved in 200 μL of 50% acetonitrile and stirred for 30 min in the dark at 25 °C. Peptides were purified by reverse-phase HPLC and lyophilized to yield Fmoc-[(4-azidosalicyl)Lys^{14}][M43A]pPSY1[43-57]. Purified peptide was further treated with 100 μL of piperidine:acetonitrile:water (2:1:1) for 15 min to remove the Fmoc groups. The deprotected peptide was purified by reverse-phase HPLC and lyophilized to obtain [(4-azidosalicyl)Lys^{14}][M43A]pPSY1[43-57] (hereafter referred as ASA-pPSY1[43-57]). ASA-pPSY1[43-57] was further radioiodinated by using the chloramine T method. ASA-pPSY1[43-57] [6.1 μg (4 nmol)], unlabeled NaI [0.07 μg (0.46 nmol)], carrier-free Na^{125}I [18.5 MBq (0.23 nmol); MP Biomedicals] and chloramine T [1.1 μg (4 nmol)] were dissolved in 50 μL of 100 mM NaH_2PO_4-NaOH buffer (pH 7.5) and stirred for 30 min in the dark at room temperature. The labeled peptide was purified by reverse-phase HPLC to yield analytically pure [^{125}I]ASA-pPSY1[43-57] with a specific radioactivity of 210 Ci/mmol.

Photoaffinity Labeling. Partially purified TPST fractions eluted from the hydroxyapatite column (30 μL) were mixed with PAP to a final concentration of 200 μM, then 40 kBq of [^{125}I]ASA-pPSY1[43-57] was added, and the mixture was incubated at 30 °C for 30 min. The mixture was irradiated on ice for 10 min with an UV lamp [model ENF-260C/J (365 nm); Spectronics) at a distance of 1 cm. For competitive replacement, the labeling experiment was performed in the presence of 20 μM of unlabeled pPSY1[43-57] peptide. Cross-linked proteins were separated by SDS/PAGE on a 10% acrylamide gel. The dried gels were exposed to a bio-imaging plate (MS 2025; Fujifilm) for 2 days at room temperature, then the plates were analyzed by using an imaging plate reader and bio-imaging analyzer (BAS 5000; Fujifilm).

PMF Analysis. After SDS/PAGE, the gel was stained with Deep Purple total protein stain (GE Healthcare) according to the manufacturer's instructions. The 62-kDa band was excised and subjected to in situ digestion with TPCK-trypsin. The resultant peptides were extracted from the gel, concentrated in vacuo, and analyzed by MALDI TOF-MS (Voyager-DE STR; Applied Biosystems, carried out by APRO Life Science Institute). The collected mass spectra were searched using the PMF program against the *Arabidopsis* database of MASCOT Matrix Science (www.matrixscience.com/).

Expression of AtTPST in Yeast. AtTPST protein was overexpressed in yeast (strain INVSc1) transformed with a pYES2 vector (Invitrogen) containing the full-length *AtTPST* cDNA sequence. Protein expression was induced in synthetic complete (SC) medium with 2% galactose at 30 °C for 16 h with continuous shaking. Yeast cells harvested from 5-mL of culture were disrupted by glass beads in 1 mL of 50 mM Tris·HCl (pH 7.5) buffer containing 1 mM DTT, 1 mM PMSF and 5% glycerol at 4 °C. The slurry was centrifuged at 3,000 $\times$ *g* for 20 min at 4 °C. The supernatant was then centrifuged at 100,000 $\times$ *g* for

30 min at 4 °C to give a pellet of microsomal membranes. For the TPST assay, 30 μg of microsomal membranes were added in the reaction buffer.

Expression Pattern of *AtTPST*. For the promoter analysis of *AtTPST*, the upstream 2.0-kb promoter region of *AtTPST* was amplified by genomic PCR, then cloned by translational fusion in-frame with the GUS coding sequence in the binary vector, pBI101. *Arabidopsis* (Col) was transformed with these constructs via *Agrobacterium tumefaciens* (C58C1), by using the standard floral dip method. Histochemical analysis of *GUS* gene expression in the transformed plants was performed as described (12).

Subcellular Localization of AtTPST. Because AtTPST has consecutive basic amino acids near the C terminus that may function as a subcellular targeting signal, we inserted GFP between the N-terminal signal peptide and the core region of AtTPST. To this end, the sequences for the N-terminal signal peptide of AtTPST and the core region of AtTPST were separately amplified from MM2d cDNA by PCR. DNA fragments corresponding to the signal peptide domain of AtTPST, GFP coding region, and the core region of AtTPST were ligated in-frame in this order between the Cauliflower mosaic virus 35S promoter and the nopaline synthase terminator of the pUC-35S:NOS vector, by using the In-Fusion cloning system (Clontech). The resulting pUC-35S:GFP-AtTPST:NOS vector was used for expression analysis. The mRFP-SYP31 expression vector was a kind gift from Takashi Ueda (University of Tokyo). PEG-mediated transient transformation of *Arabidopsis* MM2d protoplasts was carried out essentially as described previously (13). Images were collected by using a confocal laser-scanning microscope (Olympus FV300) with argon laser excitation at 488 nm or helium-neon laser excitation at 543 nm.

Analysis of *tpst-1* Mutant. The T-DNA tagged mutant, *tpst-1*, was identified in the SALK T-DNA collection (SALK_009847). The mutant was backcrossed once to WT *Arabidopsis* (Col ecotype). The site of T-DNA insertion was confirmed by genomic PCR. Total RNA was extracted from 2-week-old plants by using an RNeasy Plant Mini Kit (Qiagen). For semiquantitative RT-PCR, 2.5 μg of total RNA treated with DNase I (Invitrogen) was used to generate the first-strand cDNA, by using a First-Strand Synthesis Kit (GE Healthcare). PCR amplification was performed by using a 1-μL aliquot of a 20-μL RT reaction mixture, with 30 amplification cycles. For complementation analysis, the full-length *AtTPST* cDNA was ligated downstream of the CaMV 35S promoter in the binary vector, pIG121. The constructs were introduced into the *Arabidopsis tpst-1* mutant by *Agrobacterium*-mediated transformation. *Arabidopsis* seedlings were grown on B5 agar medium containing 1% sucrose or rockwool under continuous light at 22 °C. For root imaging, cell outlines were stained with 10 μg/mL propidium iodide for 10 min and observed under a confocal laser-scanning microscope (Olympus FV300) with helium-neon laser excitation at 543 nm. For vascular bundle imaging, leaves were fixed in a 1:9 mixture of acetic acid/ethanol and cleared in a mixture of chloral hydrate/glycerol/water (8:1:2).

ACKNOWLEDGMENTS. We thank Dr. Tomohiro Uemura and Dr. Takashi Ueda (University of Tokyo) for providing mRFP-SYP31 expression vector, and the Radioisotope Research Center of Nagoya University for instrumental support in radioisotope experiments. This work was supported by the Ministry of Education, Culture, Sports, Science, and Technology (MEXT) Scientific Research for Priority Areas Grant 19060010, the MEXT Young Scientists Grant 18687003, and the Japan Society for the Promotion of Science for Creative Scientific Research Grant 19GS0315.

1. Moore KL (2003) The biology and enzymology of protein tyrosine *O*-sulfation. *J Biol Chem* 278:24243–24246.
2. Matsubayashi Y, Sakagami Y (1996) Phytosulfokine, sulfated peptides that induce the proliferation of single mesophyll cells of *Asparagus officinalis* L. *Proc Natl Acad Sci USA* 93:7623–7627.
3. Matsubayashi Y, Ogawa M, Morita A, Sakagami Y (2002) An LRR receptor kinase involved in perception of a peptide plant hormone, phytosulfokine. *Science* 296:1470–1472.
4. Amano Y, Tsubouchi H, Shinohara H, Ogawa M, Matsubayashi Y (2007) Tyrosine-sulfated glycopeptide involved in cellular proliferation and expansion in *Arabidopsis*. *Proc Natl Acad Sci USA* 104:18333–18338.
5. Beisswanger R, et al. (1998) Existence of distinct tyrosylprotein sulfotransferase genes: Molecular characterization of tyrosylprotein sulfotransferase-2. *Proc Natl Acad Sci USA* 95:11134–11139.
6. Ouyang Y, Lane WS, Moore KL (1998) Tyrosylprotein sulfotransferase: Purification and molecular cloning of an enzyme that catalyzes tyrosine *O*-sulfation, a common post-translational modification of eukaryotic proteins. *Proc Natl Acad Sci USA* 95:2896–2901.
7. Hanai H, Nakayama D, Yang H, Matsubayashi Y, Hirota Y, Sakagami Y (2000) Existence of a plant tyrosylprotein sulfotransferase: Novel plant enzyme catalyzing tyrosine *O*-sulfation of preprophytosulfokine variants *in vitro*. *FEBS Lett* 470:97–101.
8. Matsubayashi Y, Ogawa M, Kihara H, Niwa M, Sakagami Y (2006) Disruption and overexpression of *Arabidopsis* phytosulfokine receptor gene affects cellular longevity and potential for growth. *Plant Physiol* 142:45–53.
9. Niehrs C, Huttner WB (1990) Purification and characterization of tyrosylprotein sulfotransferase. *EMBO J* 9:35–42.
10. Uemura T, et al. (2004) Systematic analysis of SNARE molecules in *Arabidopsis*: Dissection of the post-Golgi network in plant cells. *Cell Struct Funct* 29:49–65.
11. Menges M, Murray JA (2002) Synchronous *Arabidopsis* suspension cultures for analysis of cell-cycle gene activity. *Plant J* 30:203–212.
12. Kosugi S, Ohashi Y, Nakajima K, Arai Y (1990) An improved assay for β-glucuronidase in transformed cells. *Plant Sci* 70:133–140.
13. Abel S, Theologis A (1994) Transient transformation of *Arabidopsis* leaf protoplasts: A versatile experimental system to study gene expression. *Plant J* 5:421–427.